Indian Journal of Chemistry
Vol. 60A April 2021, pp. 556-560

Vapourchromic alkali metal ions complexes based on 2-phenmethylamino-7-methyl-1,8-naphthyridine

Quan-Qing Xu, Wei-Hua Mu, Zhi Yang & Feng-Yi Liu*

Faculty of Chemistry and Chemical Engineering, Yunnan Normal University, Kunming 650 050, PR China
*E-mail: qqxu1977@163.com (QQX)/ lfy20110407@163.com (FYL)

Received 21 October 2020; revised and accepted 02 March 2021

A series of 2-phenmethylamino-7-methyl-1,8-naphthyridine/alkali metal ion (Li^+ and Na^+) complexes have been synthesized using a polymeric medium (poly(acrylic acid)) as the key activating component. Upon exposure to methanol or ethanol vapour at ambient temperature, the emission colour of prepared complexes in solid powder and thin film states changes from red-orange or pink to blue, respectively. These phenomena are reversible and rapid (about 5-10 s), hence, the prepared complexes have potential applications as chemosensor materials for detection of volatile methanol vapour.

Keywords: Alkali metal ions, 1,8-Naphthyridine, Complexes, Vapourchromism, Chemosensor

Since the first reported application of fluorescence chemosensors appeared in the early 1980s[1], chemosensor research has increased tremendously. Numerous fabrication methodologies have been reported, and their applications have migrated to a variety of fields such as detection of physiologically important ions[2], monitoring of humidity[3] and pH[4] changes, and monitoring of harmful masses in the environment, especially gases such as CO_2 and methanol vapor[5,6]. The majority of studies conducted on chemosensor materials in recent decades mainly focus on small molecules[7], metal-ligand complexes[8], and doped or functional polymers[9]. These materials are highly efficient and selective, but many shortcomings still remain including difficult and tedious fabrication procedure, phase separation[10], and poor reversibility, to name a few.

1,8-Naphthyridine and its derivatives exhibit high fluorescence quantum efficiency and are readily colour-tunable compounds with multiple binding sites[11]. Additionally, they have great potential as important chemosensor materials, however, to-date, only few studies described their sensing applicability[12,13]. Furthermore, most chemosensors based on small molecular metal-ligand complexes and polymeric metal-ligand complexes, employ transition/rare earth metals such as Cu, Zn[14], Pt[8,15], Ti[16], La, Pd[10,17] etc. Few reports have applied alkali metal complexes as chemosensors. Moreover, reports examining alkali metal complexes containing naphthyridine moiety in sensors is very rare. Herein, we report a new series of Li^+/Na^+ alkali metal ion complexes based on 2-phenmethylamino-7-methyl-1,8-naphthyridine (PAMN). Preparation of the complexes involves the utilization of a polymeric intermediate, poly(acrylic acid) (PAA), as the key component. Polymer-assisted synthesis methodology has been applied in many fields, particularly in the drug synthesis[18,19,20], in which the polymers mainly act as intermediates[18], or templates[21] that can simplify the process and final purification procedure, and improve the overall output[22]. Dissolution of the prepared complexes can be achieved in various common volatile organic solvents, which facilitates the preparation of casting or spin-coated thin film devices. Furthermore, we observed that the prepared complexes exhibit individual emission colours in thin film and solid state, which can change rapidly and reversibly from red to orange or pink to blue, respectively, when exposed to methanol or ethanol vapour. Thereby, the complexes have great potential as chemosensor materials for the detection of methanol/ethanol vapour.

Materials and Methods

The total syntheses are shown in the Supplementary Data, Scheme S1 and S2. It was not possible for compound **4,** PAMN (see Scheme S1 and Fig. S1 for detail synthesis procedure) to interact directly with lithium hydroxide in methanol. PAA plays a very important role in the synthesis of complexes **6** ($MOH(PAMN)_2$, M = Li^+, complex **6a**;

M = Na^+, complex **6b**, (Scheme S2). Moreover, although sodium hydroxide can act with the compound **4** to form the crude complex **6b**, the product is expected to decompose during the purification process. The promotion behaviour of PAA in the reaction and purification process can be attributed to the polymer effect. The side chains of PAA are able to coordinate with the alkali metal ions and interact with each other and/or coil. Herein, the PAA complexes formed a complex local microenvironment in which the trapped metal ions and water molecules are easy close to the PAMN molecules. More experimental details are provided in the Supplementary Data.

Results and Discussion

As shown in Fig. 1, when the initial feed mole ratio of acrylic acid vs. PAMN is varied from 1:1 to 14:1, the high-energy emission bands centered at 442 nm and the low-energy emission bands in the region of 460-490 nm were observed upon excitation at 365 nm and the emission intensity increases gradually. The solid state PAMN displays an intense emission (λ_{max} at 401 nm). Therefore, the observed low-energy bands are tentatively assigned to the decreased π-π stacking of the PAMN molecules in the side chains of the polymeric compound when the proportion of acrylic acid in the PAA-PAMN polymer increases. The emission bands centered at 442 nm may be attributed to the formation of compound **5** (PAA-PAMN, Scheme S2).

The binding site of PAA with **4** was investigated by a quantum chemical calculation carried out at the B3LYP/6-31G(d,p) level. The calculated total energy of the molecule in which H^+ of PAA was chelated with N of 2-phenmethylamino, were -783.40984870 a.u., -783.44498231 a.u. and -783.45230834 a.u. for N1 and N8 atoms, respectively. Based on these results, the binding site was expected to be the N8 atom of compound **4**. In order to make the molecules of **4** sufficiently interact with the alkali metal ions, PAA_{14}-$PAMN_1$ was chosen, in which the compound **4** is essentially unable to interact with each other.

The structures of complexes **6a** and **6b** can be identified from the data analysis of ^1H NMR, MS, IR of **4** and **6** and Gaussian 03 DFT computation. The chemical shift of H atom of –NH– group of **4** varies from 4.00 to 7.80-7.82 and 7.79-7.82 ppm and splits into triple peaks corresponding to that of **6a** and **6b**, respectively. These changes could be attributed to the strong interaction between alkali metal ion and N atom of –NH– group. Chemical shift of other H atoms changes more or less correspondingly, before and after alkali metal ions chelation. The data of MS shows (Supplementary Data, Fig. S2) that one alkali metal ion coordinates with two PAMN molecules. The result of DFT computation indicates that when alkali metal ion coordinates with N1 and N8 atoms the conformation of complexes is optimum.

As shown in Fig. 2, the vibration of NH of complexes **6a** and **6b** locating at 3268 cm^{-1} becomes wider and blunter compared with that of **4**. This indicates the N atom form the–NH– group does not coordinate with the alkali metal ion, and it is the N1 and N8 atoms of 1,8-Naphthyridine which have a coordination relationship with the alkali metal ion. Compared with that of **4**, it also can be observed that the vibration peak intensity of C=N group locating at 1623 cm^{-1} of **6a** and 1624 cm^{-1} of **6b** increased while that locating at 1540 cm^{-1} of **6a** and 1522 cm^{-1} of **6b**

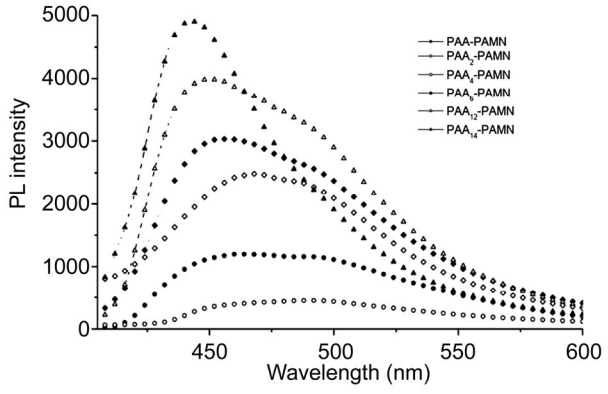

Fig. 1 — Emission spectra of PAA-PAMN solid thin films on quartz plate made by drop-coating with different feed ratio

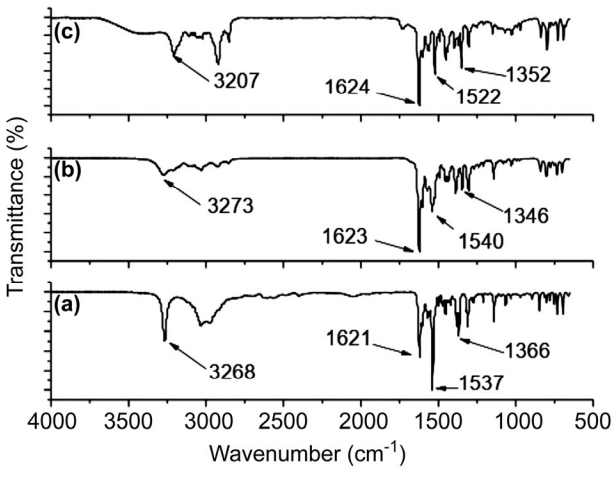

Fig. 2 —IR spectra of (a) PAMN, (b) complex **6a**, and (c) complex **6b**

decreased dramatically. Moreover, in the complexes **6,** the vibration peaks of C-N group locating at 1346 cm^{-1} of **6a** and 1352 cm^{-1} of **6b** shift to the lower wavenumber. These results indicate interactions among alkali metal ions, N1, N8 atoms as well as N atom of –NH– with each other. The complexes **6** were treated by a special procedure (see Supplementary Data). In order to facilitate the expression, the treated complexes **6** are expressed as complexes **7**. From the characteristic data of complexes **7**, it can be tentatively rationalized that complexes **6** and **7** may be in the different configurations of the same complexes.

Fig. 3 shows the UV-visible spectra of PAMN, complexes **6a**, and **6b** in methanol. From the spectra, it can be observed that **6a** and **6b** have the similar absorption spectra. As observed from the inset, the absorption spectra of these complexes in solid film are slight different from the absorption spectra in methanol. The absorption band of **6** is red-shifted from 366 nm of PAMN to 376 nm. The band may be assigned to the electronic density of the PAMN rings which is subsequently redistributed around the coordination sites between the N1 and N8 atoms with $Li^{+}(Na^{+})$. So, the decrease of energy gap results in the red-shift of the absorption band. The PAA-PAMN exhibits the similar absorption trace to that of PAMN. Fig. 4 shows the absorption spectra of PAMN, complexes **7a**, **7b** in DMSO solution and the inset is the spectra of their thin solid films on quartz plates. These compounds have the similar absorption spectra in solution. However, the absorption bands of **7a** and **7b** films blue-shifted from 367 nm of PAMN to 342 nm and 347 nm, respectively. This may due to the molecules of complexes **7** can interact more strongly with each other, under the formation of intermolecular hydrogen bonding after removing the dimethyl sulfoxide solvent.

Upon excitation at 365 nm, solid films of **6a** and **6b** display high- and low-energy emission bands at about 430 nm and 580 nm at room temperature (Figs 5 and 6). Compared with emission of the solid PAMN thin film, the high-energy band was

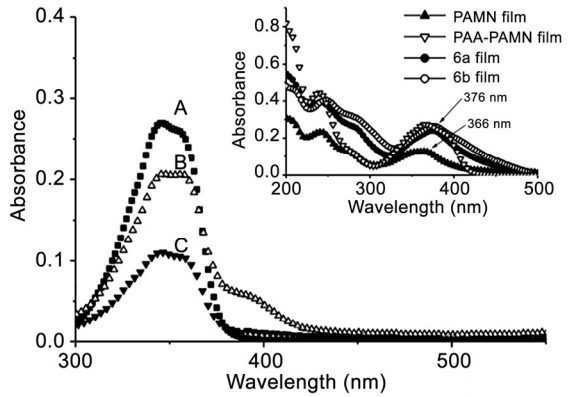

Fig. 3 — UV-visible absorption spectra of (A) **6a**, (B) **6b**, (C) PAMN, in methanol; Inset: The absorption spectra of 6a (●) and 6b(○), PAMN(▲), PAA-PAMN(▽) in solid thin film on quartz plate

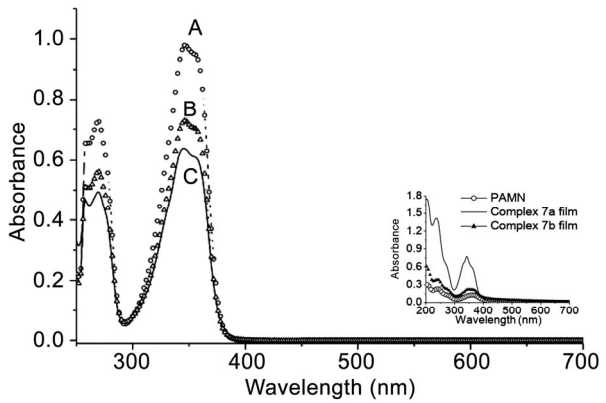

Fig. 4 — UV-visible absorption spectra of (A) PAMN, (B) complex **7a**, and (C) complex **7b** in DMSO. Inset: The absorption spectra of their solid films on quartz plates

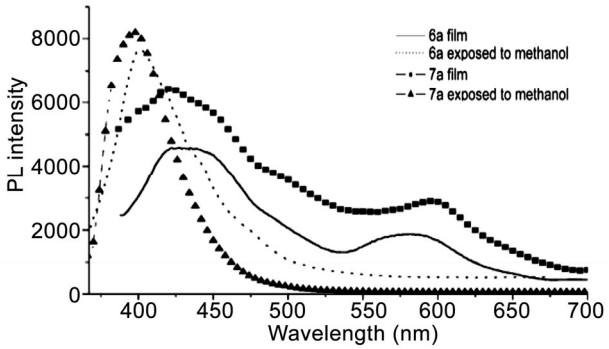

Fig. 5 — Emission spectra of **6a** and **7a** solid films on quartz plate

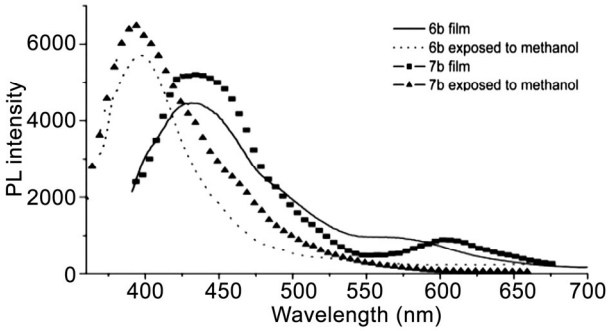

Fig. 6 — Emission spectra of **6b** and **7b** solid films on quartz plate fabricated by drop-coating and the emission spectra of them exposed to methanol vapour

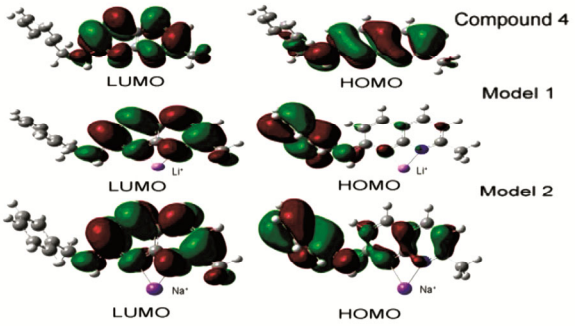

Fig. 7 — Contour plots of calculated HOMO and LUMO orbitals of the compound 4 and model complexes of 6: Model 1 (**6a**), Model 2 (**6b**)

red-shifted (30 nm). These can be attributed to the interaction of N atoms of 2-phenmethylamino moiety with Li^+ or Na^+, which make the electron clouds density of PAMN rings redistribute to decrease the energy gap. As shown, **6a** and **6b** exhibit emission maxima centered at 398 nm when the complexes are exposed to the methanol vapour. The interaction among Li^+ or Na^+, N atoms of PAMN are interrupted by many methanol molecules, leading to the blue-shift of emission peaks. Complexes **7** exhibit a similar behaviour with **6** when excitated at 365 nm or exposed to methanol vapour. However, the emission maxima of low-energy bands of are observed at about 601 nm (Fig. 6).

In order to reveal the nature of low-energy emission bands caused by alkali metal ions, a quantum chemical calculation was performed by two simplified model complexes, and carried out at the B3LYP/6-31G(d,p) level, before and after alkali metal ions chelation. From Fig. 7, it can be observed that in model complexes, the alkali metal ions do not participate in the formation of the frontier molecular orbitals (MOs), but do induce a redistribution of electron clouds density of the frontier MOs acting as a point charge. The electron clouds of HOMO orbital of compound **4** mainly localize on the naphthyridine ring. However, with the addition of Li^+ or Na^+, the electron clouds of HOMO orbitals mainly transfer from the naphthyridine ring to the benzene ring gradually. Although the electron clouds intensity of LUMO of them remain without much change, the phase of electron clouds is reverse when compared with that of compound **4**. These indicate a charge-transfer (CT)[23] state character in the complexes **6**. The calculation of energy gap demonstrates a drop in energy levels and a drop in corresponding energy gaps of them for the chelation of alkali metal ions.

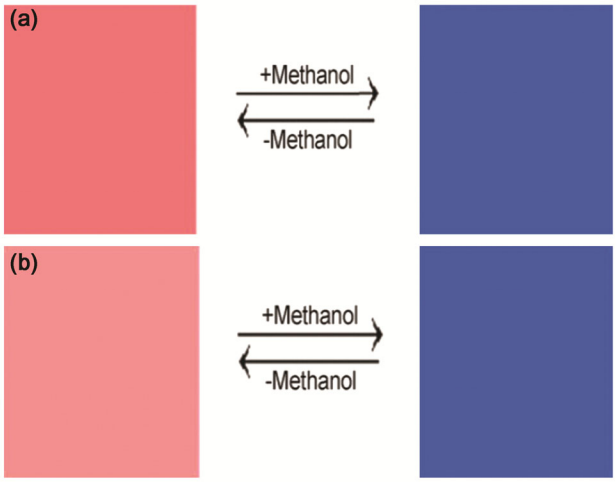

Fig. 8 — Vapourchromism of (a) **6a** and (b) **6b** solid film on quartz plate fabricated by drop-coating (excited at 365 nm)

The ΔE (a.u.) (E_{LUMO}, E_{HOMO}) of **4**, model complexes of **6a** and **6b** are 0.161 (-0.045,-0,206), 0.147 (-0.189, -0.336) and 0.153 (-0.178, -0.331), respectively. Therefore all the high-energy emission bands of **6** are red-shifted compared with that of **4**. Furthermore the chelation of Li^+ or Na^+ with PAMN induces a red low-energy emission band.

Photoluminescence responses of **6a** and **6b** towards methanol vapour were investigated. The spin-coated films **6a** and **6b** were prepared by spin coating method, and their detection experiments on alcohol vapour are shown in the Supplementary Data. A substantial changes of emission colour from red-orange (Fig. 8a) and pink (Fig. 8b) to blue were observed for Li^+ and Na^+ complexes, respectively. Complexes **7a** and **7b** display dark-red and red-orange emissions and exhibit the similar changes of emission colour under same condition. The vapourchromism process is rapid (about 5-10 seconds) and reversible. However, the influences of water molecules upon the nature of emissive state of **6** and **7** are completely different. Complexes **6** also achieve vapourchromism when exposing to water vapour, but for complexes **7,** it is not observed.

Conclusions

A new series of PAMN complexes with alkali metal ions have been synthesized. Upon exposure to methanol or ethanol vapour, the emission colours of the complexes thin films transform from red to orange or pink to blue, respectively. These phenomena are reversible and rapid. Complex **7** displays a superior selectivity than complex **6**. The studied complexes

have potential as chemosensor materials for the detection of alcohol vapours.

Supplementary Data

Supplementary data associated with this article are available in the electronic form at http://nopr.niscair.res.in/jinfo/ijca/IJCA_60(04)556-560_SupplData.pdf.

Acknowledgement

This work was supported by the National Natural Science Foundation of China (21162043, 21565033, 21901227).

References

1 Grynkiewicz G, Poenie M & Tsien R Y, *J Biol Chem*, 260 (1985) 3440.
2 Spichiger-Keller U E, *Chemical Sensors and Biosensors for Medical and Biological Applications*, (Wiley-VCH, New York) 1998.
3 Casalbore-Miceli G, Yang M J, Li Y, Zanelli A, Martelli A, Chen S, She Y & Camaioni N, *Sens Actuators B*, 114 (2006) 584.
4 Sebra R P, Kasko A M, Anseth K S & Bowman C N, *Sens Actuators B*, 119 (2006) 127.
5 Kim S, Prajitno H, Yoo J, Kim S, Chun D, Lim J, Choi H, Lee S & Im H, *J Ind Eng Chem*, 94 (2021) 317.
6 Stevens N &Akins D L, *Sens Actuators B*, 123 (2007) 59.
7 Hu R, Zhang X, Xu Qiang, Lu D Q, Yang Y H, Xu Q Q, Ruan Q, Mo L T & Zhang X B, *Biosens Bioelectron,* 92 (2017) 40.
8 Wadas T J, Wang Q M, Kim Y J, Flaschenreim C, Blanton T N & Eisenberg R, *J Am Chem Soc*, 126 (2004) 16841.
9 Tew G N, Aamer K. A & Shunmugam R, *Polymer*, 46 (2005) 8440.
10 Wolfbeis O S, *J Mater Chem,* 15 (2005) 2657.
11 Maekawa M, Munakata M, Kitagawa S, Kuroda-Sowa T, Suenaga Y & Yamamoto M, *Inorg Chim Acta*, 271 (1998) 129.
12 Nakatani K, Horie S & Saito I, *J Am Chem Soc*, 125 (2003) 8972.
13 Liao J H, Chen C T, Chou H C, Cheng C C, Chou P T, Fang J M, Slanina Z & Chow T J, *Org Lett*, 4 (2002) 3107.
14 Spadavecchia J, Ciccarella G, Siciliano P, Capone S, & Rella R, *Sens Acutuators B*, 100 (2004) 88.
15 Kwok C C, Yu S C, Sham I H T. & Che C M, *Chem Commun*, (2004) 2512.
16 Kim H S, Moon W T, Jun Y K, & Hong S H, *Sens Acutuators B*, 120 (2006) 63.
17 Siemons M & Simon U, *Sens Acutuators B*, 120 (2006) 110.
18 Li X, Abell C, Warrington B H & Ladlow M, *Org Biomol Chem*, 1 (2003) 4392.
19 Bapna A, Vickerstaffe E, Warrington B H, Ladlow M, Fan T P & Ley S V, *Org Biomol Chem*, 2 (2004) 611.
20 Chen M, Pan L J, Cao J M, Ji H M, Ji G B, Ma X J & Zheng Y D, *Mater Lett*, 60 (2006) 3842.
21 El-Rehim H A, Hegazy E A, Khalil F H & Hamed N A, *Nucl Instrum Methods Phys Res B*, 254 (2007) 105.
22 Yang G C, Chen Z X. & Zhang H Q, *Green Chem*, 5 (2003) 441.
23 Tian L L, Zhang W, Yang B, Lu P, Zhang M, Lu D, Ma Y G & Shen J C, *J Phys Chem B*, 109 (2005) 6944.